

Ligand Steric Contours To Understand the Effects of *N*-Heterocyclic Carbene Ligands on the Reversal of Regioselectivity in Ni-Catalyzed Reductive Couplings of Alkynes and Aldehydes

Peng Liu,[†] John Montgomery,^{*,‡} and K. N. Houk^{*,†}

[†]Department of Chemistry and Biochemistry, University of California, Los Angeles, California 90095-1569, United States

[‡]Department of Chemistry, University of Michigan, Ann Arbor, Michigan 48109-1055, United States

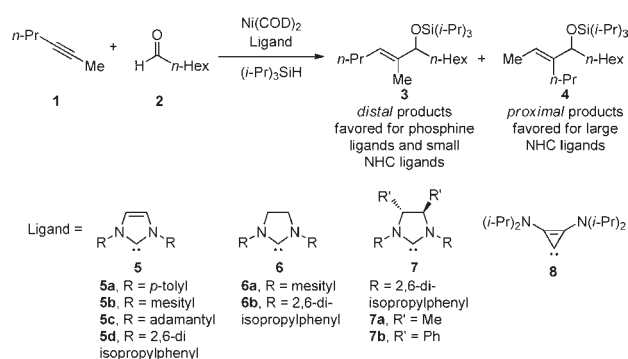
S Supporting Information

ABSTRACT: The regioselectivities of *N*-heterocyclic carbene (NHC) ligands in Ni-catalyzed alkyne–aldehyde reductive coupling reactions with silane reducing agents are investigated using density functional theory. Reversal of regioselectivity can be achieved by varying the steric bulkiness of the ligand. The steric influences of NHC ligands are highly anisotropic. Regioselectivity is primarily controlled by the steric hindrance at the region of the ligand close to the alkyne. Analysis of 2D contour maps of the NHC ligands indicates that the regioselectivities are directly affected by the shape and orientation of the *N*-substituents on the ligand.

The control of regiochemistry is a widespread challenge in addition reactions to nonpolar π -systems such as alkenes, alkynes, dienes, and allenes. Substrates that lack strong steric or electronic biases typically undergo regiochemically unselective additions, whereas regiocontrol with more biased substrates, while sometimes selective, often cannot be reversed. Regiochemical reversals are sometimes accomplished by employing substrate direction strategies,¹ by employing two fundamentally distinct procedures,² or by altering the mechanism³ or rate-determining step⁴ of the process. Recently, Montgomery and co-workers reported that dramatic regiochemical reversals in a broad range of aldehyde–alkyne reductive coupling processes were possible by tuning the size of *N*-heterocyclic carbene (NHC) ligands (Scheme 1).^{5,6} Given uncertainties in the origin of this effect, we have set out to determine if the regiochemical reversals arise from steric effects in a common mechanistic pathway, or from a fundamental change in the mechanism or rate-determining step of the additions.⁷ Furthermore, elucidating the precise nature of the requisite interactions will guide the design of more effective catalysts and the identification of other reaction classes that allow regiocontrol by NHC ligand variation.

A widely recognized model to describe the steric properties of NHC ligands involves the “buried volume” ($\%V_{\text{bur}}$), defined as the percentage of volume occupied by the ligand in the first coordination sphere of the metal.⁸ $\%V_{\text{bur}}$ is a measurement of average bulkiness of the ligand. In contrast, regioselectivities are often controlled by interactions between substrates and specific regions of the ligand. Especially, factors such as the orientation and conformation of the *N*-substituents (wingtips) on the NHC ligands may be essential for regiochemical control,^{9,10} while $\%V_{\text{bur}}$ is not sensitive to these effects.¹¹

Scheme 1. Ni-Catalyzed Reductive Couplings of Alkynes and Aldehydes with *N*-Heterocyclic Carbene Ligands⁵



We report the first theoretical study on the regioselectivities of Ni-catalyzed reductive alkyne–aldehyde coupling reactions with NHC ligands (Scheme 1). Density functional theory calculations provide good agreement with experimental regioselectivities across the range of ligands examined. We find that regioselectivity is controlled by steric repulsion between the alkyne substituents and the highly hindered NHC ligand in the oxidative addition transition state (TS).¹² The regioselectivities are directly affected by the shape and orientation of the *N*-substituents on the NHC ligand, which we illustrate through the use of steric contours of ligands.

The mechanism and regioselectivities of Ni-catalyzed alkyne–aldehyde couplings using phosphine ligand and organoborane as reductant were previously investigated.¹³ The regioselectivity of couplings of alkynes without directing groups is controlled by steric repulsions around the forming C–C bond in the oxidative addition TS, leading to C–C bond formation at the less hindered terminus of the alkyne. Similar to the reactions with phosphine ligands, the rate- and regioselectivity-determining step, irrespective of NHC size, is the oxidative addition of alkyne and aldehyde to form a five-membered metallacycle intermediate.¹⁴ In the oxidative addition TS, the Ni, alkyne, aldehyde, and the carbene carbon atom are all in the same plane. The imidazolylidene ring is perpendicular to this plane. This conformation minimizes the steric repulsions of

Received: March 4, 2011

Published: April 20, 2011

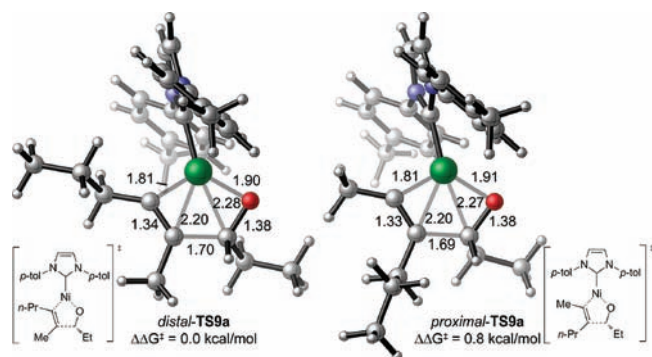


Figure 1. Oxidative addition transition states with ligand 5a.

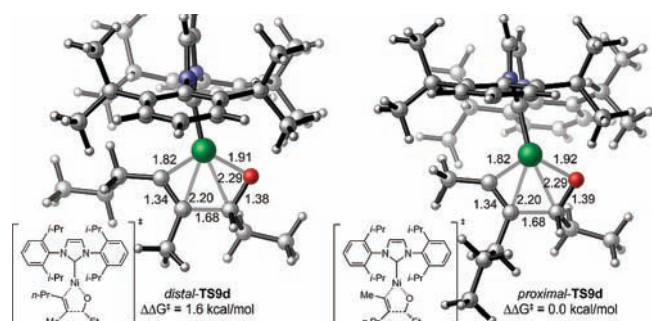


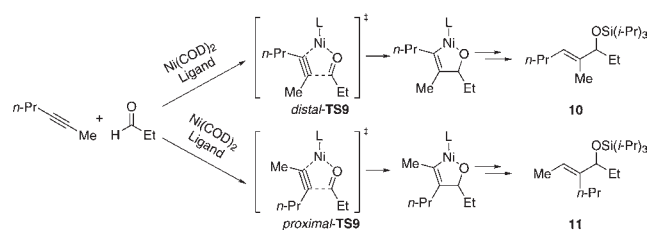
Figure 2. Oxidative addition transition states with ligand 5d.

the ligand with the substrates. Two different orientations are possible for unsymmetrical alkynes in the oxidative addition TS, leading to the two regioisomeric products (Figures 1 and 2). Here we define the *distal* pathway as that in which the bulkier alkyne substituent is distal to the forming C–C bond in the TS. The *proximal* pathway has the bulkier alkyne substituent proximal to the forming C–C bond. The regioselectivities of these coupling reactions are determined by the energy differences between the *distal* and *proximal* oxidative addition TSs.

The regioselectivities of the couplings of 2-hexyne and propionaldehyde with several NHC ligands were calculated in Gaussian 09¹⁶ using two levels of theory: (a) geometry optimizations and frequency calculations using B3LYP¹⁷ with a mixed basis set of LANL2DZ for Ni and 6-31G(d) for other atoms; and (b) single-point calculations using the B3LYP optimized geometry with the M06¹⁸ functional and a larger basis set of SDD for Ni and 6-311+G(d,p) for other atoms. The predicted differences in activation enthalpies and Gibbs free energies at 298 K between *distal* and *proximal* pathways are shown in Table 1. Both B3LYP and M06 calculations provide good agreement with the experimental regioselectivities. In general, M06 single-point calculations provide slightly superior results to B3LYP. B3LYP predicted the wrong major regioisomers for reactions with ligands 5b and 6a, while the M06 results agree with the experiment. The predicted ratios of the distal and proximal products are calculated on the basis of the differences in free energies from M06 calculations. They agree very well with experimental ratios for all ligands investigated.

The buried volumes of the ligands are also given in Table 1.¹⁵ Although there is a qualitative trend toward increasing preference for 11 and larger % V_{bur} , the correlation is not quantitative, and there are many exceptions to the trend. For example, the adamantyl-substituted ligand 5c has the second largest % V_{bur} ,

Table 1. Calculated Regioselectivities in Couplings of 2-Hexyne and Propionaldehyde



ligand ^a	% V_{bur} ¹⁵	B3LYP ^c		M06 ^{b,c}		ratio	
		$\Delta\Delta H^\ddagger$	$\Delta\Delta G^\ddagger$	$\Delta\Delta H^\ddagger$	$\Delta\Delta G^\ddagger$	predicted ^d	exptl ^e
5a	30.5	0.4	0.5	0.5	0.8	79:21	87:13
8	24.9	0.0	0.3	0.3	0.4	64:36	86:14
5b	31.6	−0.3	−0.5	0.3	0.2	57:43	67:33
6a	32.7	−0.4	−0.5	0.1	0.2	59:41	61:39
5c	36.1	−0.8	−0.6	−1.4	−1.2	11:89	44:56
5d	33.6	−1.9	−1.5	−0.9	−1.6	6:94	20:80
6b	35.7	−2.1	−3.4	−0.8	−1.9	4:96	7:93
7a	38.9	−2.7	−3.1	−3.0	−3.4	1:99	6:94 ^f

^a For structures of these ligands, see Scheme 1. ^b Zero-point energies, thermal corrections, and entropies are calculated at the B3LYP/LANL2DZ–6-31G(d) level. ^c Activation energy differences are defined as (*proximal* – *distal*). Energies are in kcal/mol. Gibbs free energies are calculated at 298 K. ^d Ratio of 10:11 calculated from M06 Gibbs free energies. ^e Heptanal is used in place of propionaldehyde in the experiment. See ref 5. ^f Ligand 7b ($R' = \text{Ph}$) is used in place of 7a ($R' = \text{Me}$) in the experiment.

while its regioselectivity is low. The 2,6-diisopropylphenyl-substituted NHC ligands 5d, 6b, 7a, and 7b are much more selective for the proximal products, although their % V_{bur} values are only slightly higher than those for other ligands that lead to different regiochemical control. This type of deviation is not unexpected, since % V_{bur} describes only the average bulkiness of the ligand, while the regioselectivity is mainly determined by the steric hindrance in the region adjacent to the alkyne substituent.

The oxidative addition TS structures with ligands 5a and 5d are shown in Figures 1 and 2, respectively. For the reactions involving ligand 5a, few steric interactions between the ligand and the alkyne substituents are observed. Due to the short C–C distance in the TS (~ 1.70 Å), strong steric repulsions are expected around the forming C–C bond and thus dominate the regioselectivity of the preferred distal products. When 2,6-diisopropylphenyl-substituted NHC ligands such as 5d, 6b, and 7 are used, steric repulsions between the alkyne substituent and the ligand become significant and reverse the regiochemical preferences of the coupling products. The bulkier substituents are now oriented proximal to the forming C–C bond.

To better illustrate the steric repulsions at different regions of the ligand, 2D contour maps along the z axis¹⁹ of the van der Waals surface of ligands 5a, 5c, and 5d are plotted in Figure 3.²⁰ The corresponding CPK model diagrams are also shown. The ligand geometries are taken from a model TS structure of couplings of acetylene and formaldehyde. In ligand 5d, the atoms closest to the substrates and with the most steric hindrance (labeled in red) are on the *o*-isopropyl substituents on the phenyl group. This highly hindered region is very close to the distal

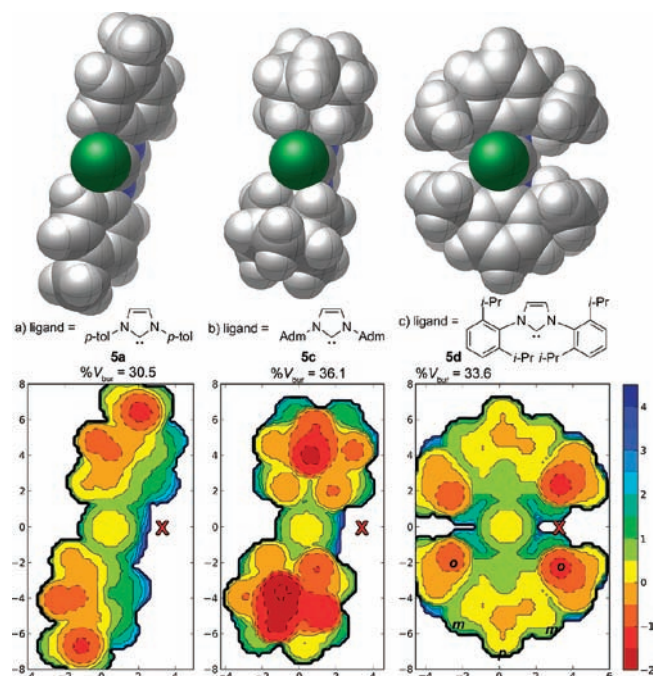
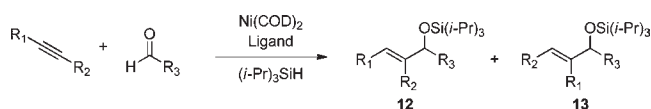


Figure 3. CPK model and 2D contour maps of the van der Waals surface of ligands **5a**, **5c**, and **5d**. Distances are in Å. Ni is located at the origin of the coordinate system in the contour maps and is shown in green in the CPK models. Contour line of zero is defined as in the same plane of the Ni atom. Negative distance (red) indicates the ligand is closer to substrate; positive distance (blue) indicates the ligand is farther away from substrate. The position of the distal alkyne substituent is marked with “X”. The regions of the *ortho*, *meta*, and *para* substituents on ligand **5d** are marked with “o”, “m”, and “p”, respectively.

alkyne substituent (labeled “X”).²¹ Similarly, the strong steric control by *o*-isopropylphenyl-substituted ligands **6b**, **7a**, and **7b** is also attributed to the bulky *ortho* substituents. In contrast, *meta* and *para* groups on the ligand are quite far away from the distal alkyne substituent and are expected to have minimal impacts on regioselectivity. Although the adamantyl-substituted ligand **5c** is very bulky with a large % V_{bur} , the most hindered region is around the adamantyl group, which is pointing away from the plane of alkyne and aldehyde (Figure 3b). The steric repulsions in the region of the distal alkyne substituent are only moderate. This explains the moderate regioselectivities observed in the couplings with ligand **5c**. The conformation of the substituents on the ligand is also important to maintain the steric control. The *o*-isopropyl groups in ligand **5d** fix the conformation of the *N*-substituted aryl groups perpendicular to the imidazolylidene ring and bring the isopropyl groups into close proximity with the distal alkyne substituent. In contrast, in ligand **5a**, the *N*-substituted *p*-tolyl groups are tilted away from the distal alkyne substituent, and no steric interactions are observed with the alkyne substrate.

The proximal products are slightly more favorable for couplings with saturated NHC ligands (**6a**, **6b**) than those with the unsaturated NHC ligands with the same R group (**5b**, **5d**, respectively). This is attributed to the shorter distances between Ni and the saturated NHC ligands, which lead to greater steric bulk of the ligands. For example, the Ni–C_{carbene} distances in *distal*-TS9 are 1.835 and 1.843 Å for ligands **6b** and **5d**,

Table 2. Calculated Regioselectivities in Couplings of Various Alkynes and Aldehydes with Ligands **8**, **5b**, **6b**, and **7a**



entry	R ₁	R ₂	R ₃	predicted ratio 12:13 ^a			
				L = 8	L = 5b	L = 6b	L = 7a
1	<i>n</i> -Pr	Me	Me	68:32	48:52	4:96	2:98
2	<i>n</i> -Pr	Me	Et	64:36	57:43	4:96	1:99
3	<i>n</i> -Pr	Me	Ph	88:12	70:30	2:98	6:94
4	<i>i</i> -Pr	Me	Ph	98:2 ^b	43:57	5:95 ^b	2:98
5	<i>i</i> -Pr	H	Et	99:1	95:5	26:74	5:95

^a Product ratios are calculated from M06 single-point energies with B3LYP zero-point energies, entropies, and thermal corrections to Gibbs free energies. ^b Entry 4 data for ligands **8** and **6b** closely match experimental data (97:3 and 10:90, respectively). For these data and the closest comparisons for the other entries, see ref 5.

respectively. Substituents on the backbone (**7a**) also increase the regioselectivity, leading to the proximal products.

The effects of substituents on alkynes and aldehydes were also investigated (Table 2). Substituents on the aldehyde have small effects on regioselectivities (entries 1–3). The backbone-substituted ligand **7a** is predicted to give greater regioselectivity of proximal products than ligand **6b** for most alkynes, especially for terminal alkynes (entry 5). The non-parallel orientation of the two *N*-aryl groups enforced by the C2 structure of ligands **7a/7b** puts the *o*-isopropyl substituents in the best position to differentiate between the substituents of terminal alkynes.²²

In conclusion, the origin of regiochemical reversal in aldehyde–alkyne reductive couplings using silane reducing agents and nickel–NHC catalysts has been established by computational methods. The control of regioselectivity by ligands derives from alkyne–ligand interactions when large ligands are employed, and from aldehyde–alkyne interactions when small ligands are employed, involving the rate-determining oxidative addition. The regiochemical reversal is unique to NHC ligands in this reaction class among the ligands studied to date. While % V_{bur} serves as a useful guide for predicting ligand steric effects, this study illustrates that regiochemistry predictions require an understanding of the precise substrate positioning adjacent to the non-uniform shape of NHC ligand. Steric contour maps of ligands provide insights into the origins of the regiochemical effects in these catalytic processes.

■ ASSOCIATED CONTENT

S Supporting Information. Optimized Cartesian coordinates and energies, details of computational methods, 2D steric contour maps for all ligands, and complete ref 16. This material is available free of charge via the Internet at <http://pubs.acs.org>.

■ AUTHOR INFORMATION

Corresponding Author

houk@chem.ucla.edu; jmontg@umich.edu

ACKNOWLEDGMENT

We are grateful to the National Science Foundation (CHE-0548209, K.N.H.) and the National Institutes of Health (GM-57014, J.M.) for financial support of this research. J.M. thanks Hasnain Malik and Grant Sormunen for helpful discussions. Calculations were performed on the National Science Foundation Terascale Computing System at the NCSA and the Hoffman2 cluster at UCLA.

REFERENCES

- (1) (a) Hoveyda, A. H.; Evans, D. A.; Fu, G. C. *J. Am. Chem. Soc.* **1993**, *93*, 1307. (b) Miller, K. M.; Jamison, T. F. *J. Am. Chem. Soc.* **2004**, *126*, 15342. (c) Bahadoor, A. B.; Flyer, A.; Micalizio, G. C. *J. Am. Chem. Soc.* **2005**, *127*, 3694. (d) Reichard, H. A.; McLaughlin, M.; Chen, M. Z.; Micalizio, G. C. *Eur. J. Org. Chem.* **2010**, 391. (e) Liu, P.; Sirois, L. E.; Cheong, P. H.-Y.; Yu, Z.-X.; Hartung, I. V.; Rieck, H.; Wender, P. A.; Houk, K. N. *J. Am. Chem. Soc.* **2010**, *132*, 10127–10135.
- (2) This strategy is exemplified by the acid-catalyzed hydration of olefins compared with hydroboration–oxidation protocols.
- (3) (a) Hein, J. E.; Fokin, V. V. *Chem. Soc. Rev.* **2010**, *39*, 1302. (b) Boren, B. C.; Narayan, S.; Rasmussen, L. K.; Zhang, L.; Zhao, H. T.; Lin, Z. Y.; Jia, G. C.; Fokin, V. V. *J. Am. Chem. Soc.* **2008**, *130*, 8923.
- (4) Ohmura, T.; Oshima, K.; Taniguchi, H.; Sugimoto, M. *J. Am. Chem. Soc.* **2010**, *132*, 12194.
- (5) Malik, H. A.; Sormunen, G. J.; Montgomery, J. J. *J. Am. Chem. Soc.* **2010**, *132*, 6304.
- (6) Reviews of Ni-catalyzed reductive alkyne–aldehyde couplings: (a) Montgomery, J. *Acc. Chem. Res.* **2000**, *33*, 467. (b) Ikeda, S. *Angew. Chem. Int. Ed.* **2003**, *42*, 5120. (c) Montgomery, J. *Angew. Chem. Int. Ed.* **2004**, *43*, 3890. (d) Montgomery, J.; Sormunen, G. J. In *Metal Catalyzed Reductive C–C Bond Formation: A Departure from Preformed Organometallic Reagents*; Krische, M. J., Ed.; Springer: Berlin/Heidelberg, 2007; pp 1–23. (e) Moslin, R. M.; Miller-Moslin, K.; Jamison, T. F. *Chem. Commun.* **2007**, 4441. For leading references with other metals, see: (f) Skukcas, E.; Ngai, M.-Y.; Komanduri, V.; Krische, M. J. *Acc. Chem. Res.* **2007**, *40*, 1394. (g) Bower, J. F.; Kim, I. S.; Patman, R. L.; Krische, M. J. *Angew. Chem. Int. Ed.* **2009**, *48*, 34.
- (7) Other notable recent examples of regiochemical reversals: (a) Gao, F.; Hoveyda, A. H. *J. Am. Chem. Soc.* **2010**, *132*, 10961. (b) Wu, J. Y.; Moreau, B.; Ritter, T. *J. Am. Chem. Soc.* **2009**, *131*, 12915.
- (8) (a) Hillier, A. C.; Sommer, W. J.; Yong, B. S.; Petersen, J. L.; Cavallo, L.; Nolan, S. P. *Organometallics* **2003**, *22*, 4322. (b) Dorta, R.; Stevens, E. D.; Scott, N. M.; Costabile, C.; Cavallo, L.; Hoff, C. D.; Nolan, S. P. *J. Am. Chem. Soc.* **2005**, *127*, 2485. (c) Cavallo, L.; Correa, A.; Costabile, C.; Jacobsen, H. J. *Organomet. Chem.* **2005**, *690*, 5407. (d) Clavier, H.; Nolan, S. P. *Chem. Commun.* **2010**, 46, 841.
- (9) The effects of *N*-substituents on the flexibility and conformations of NHC ligands were investigated in a recent dynamical study: Ragone, F.; Poater, A.; Cavallo, L. *J. Am. Chem. Soc.* **2010**, *132*, 4249.
- (10) The conformational flexibility of NHC ligands can facilitate some Pd-catalyzed cross-coupling reactions: Wurtz, S.; Glorius, F. *Acc. Chem. Res.* **2008**, *41*, 1523.
- (11) For an illustration of how stereoselective olefin polymerizations can be evaluated by % V_{bur} , see: Poater, A.; Cavallo, L. *Dalton Trans.* **2009**, 8878.
- (12) For an early illustration of regiocontrol imparted by NHC size in a Ni-catalyzed cyclization, see: Tekavec, T. N.; Arif, A. M.; Louie, J. *Tetrahedron* **2004**, *60*, 7431.
- (13) (a) McCarren, P. R.; Liu, P.; Cheong, P. H.-Y.; Jamison, T. F.; Houk, K. N. *J. Am. Chem. Soc.* **2009**, *131*, 6654. (b) Liu, P.; McCarren, P. R.; Cheong, P. H.-Y.; Jamison, T. F.; Houk, K. N. *J. Am. Chem. Soc.* **2010**, *132*, 2050. (c) Theoretical study of Rh-catalyzed hydrogenative couplings: Liu, P.; Krische, M. J.; Houk, K. N. *Chem. Eur. J.* **2011**, *17*, 4021. (d) Review of theoretical studies of regioselectivity of C–C bond-forming reactions: Liu, P.; Houk, K. N. *Inorg. Chim. Acta* **2011**, *369*, 2.
- (14) (a) The full catalytic cycle of Ni-catalyzed alkyne–aldehyde couplings using NHC ligand and organosilane as reductant was calculated using B3LYP/LANL2DZ–6-31G(d) and is included in the Supporting Information. (b) Kinetic study of Ni(NHC)-catalyzed ynal cyclizations using organosilane reductant is also consistent with the oxidative cyclization mechanism: Baxter, R. D.; Montgomery, J. J. *J. Am. Chem. Soc.* **2011**, *133*, 5728–5731.
- (15) (a) The buried volume is calculated using the SambVca program based on geometries from DFT-optimized (NHC)Ir(CO)₂-Cl complexes. See Supporting Information for details of % V_{bur} calculations. (b) Poater, A.; Cosenza, B.; Correa, A.; Giudice, S.; Ragone, F.; Scarano, V.; Cavallo, L. *Eur. J. Inorg. Chem.* **2009**, 1759.
- (16) Frisch, M. J.; *Gaussian 09*, Revision B.01; Gaussian, Inc.: Wallingford, CT, 2010.
- (17) (a) Becke, A. D. *J. Chem. Phys.* **1993**, *98*, 5648. (b) Lee, C.; Yang, W.; Parr, R. G. *Phys. Rev. B* **1988**, *37*, 785.
- (18) (a) Zhao, Y.; Truhlar, D. G. *Theor. Chem. Acc.* **2008**, *120*, 215. (b) Zhao, Y.; Truhlar, D. G. *Acc. Chem. Res.* **2008**, *41*, 157.
- (19) The *z* axis is defined as the axis along the center of the forming C–C bond and the Ni atom.
- (20) (a) For a related theoretical study of 2D contour plots of NHC ligands, see ref 9. (b) For use of steric maps to rationalize enantioselective conjugate additions, see: Poater, A.; Ragone, F.; Mariz, R.; Dorta, R.; Cavallo, L. *Chem. Eur. J.* **2010**, *16*, 14348.
- (21) “X” is the position of the carbon atom on the distal alkyne substituent that is directly bonded to the triple bond.
- (22) This could be observed in the steric contours of these ligands; see Supporting Information for details.

NOTE ADDED AFTER ASAP PUBLICATION

In the version published ASAP April 20, 2011, structure 11 in Table 1 was incorrect. The corrected version was reposted May 4, 2011.